Wharton's Jelly-derived multifunctional hydrogels: new tools for the treatment of intervertebral disc degeneration

Letizia Penolazzi[1], Anna Chierici[1], Maria Pina Notarangelo[1], Beatrice Dallan[2], Gina Lisignoli[3], Elisabetta Lambertini[1], Pantaleo Greco[4], Roberta Piva[1], Claudio Nastruzzi[2]

[1]Department of Neuroscience and Rehabilitation, University of Ferrara, Ferrara, Italy

[2]Department of Chemical, Pharmaceutical and Agricultural Sciences, University of Ferrara, Ferrara, Italy

[3]IRCCS Istituto Ortopedico Rizzoli, Laboratorio di Immunoreumatologia e Rigenerazione Tissutale, Bologna, Italy

[4]Obstetrics and Gynecology Unit, Department of Medical Sciences, University of Ferrara, Ferrara, Italy

Correspondence

Letizia Penolazzi, Department of Neuroscience and Rehabilitation, University of Ferrara, 44121 Ferrara, Italy

Claudio Nastruzzi, Department of Chemical, Pharmaceutical and Agricultural Sciences, University of Ferrara, 44121 Ferrara, Italy

Letizia Penolazzi, pnlmlt@unife.it

Anna Chierici, anna.chierici@edu.unife.it

Maria Pina Notarangelo, ntrmpn@unife.it

Beatrice Dallan, beatrice.dallan@unife.it

Gina Lisignoli, gina.lisignoli@ior.it

Elisabetta Lambertini, lmblbt@unife.it

Pantaleo Greco, pantaleo.greco@unife.it

Roberta Piva, piv@unife.it

Claudio Nastruzzi, nas@unife.it

Abstract

The degeneration of intervertebral disc (IVD) is a disease of the entire joint between two vertebrae in the spine caused by loss of extracellular matrix (ECM) integrity, to date with no cure. The various regenerative approaches proposed so far have led to very limited successes. An emerging opportunity arises from the use of decellularized ECM as a scaffolding material that, directly or in combination with other materials, has greatly facilitated the advancement of tissue engineering. Here we focused on the decellularized matrix obtained from human umbilical cord Wharton's jelly (DWJ) which retains several structural and bioactive molecules very similar to those of the IVD extracellular matrix. However, being a viscous gel, DWJ has limited ability to retain ordered structural features when considered as architecture scaffold. To overcome this limitation, we produced DWJ-based multifunctional hydrogels, in form of 3D millicylinders containing different percentage of alginate, a seaweed-derived polysaccharide, and gelatin, denatured collagen, which may impart mechanical integrity to the biologically active DWJ. The developed protocol, based on a freezing step, leads to the consolidation of the entire polymeric dispersion mixture, followed by an ionic gelation step and a freeze-drying process. Finally, a porous, stable, easily storable and suitable matrix for ex-vivo experiments was obtained. The properties of the millicylinders (WJMs) were then tested in culture of degenerated IVD cells isolated from disc tissues of patients undergoing surgical discectomy. We found that WJMs with the highest percentage of DWJ were effective in supporting cell migration, restoration of the IVD phenotype (increased expression of Collagen type 2, aggrecan, Sox9 and FOXO3a), anti- inflammatory action, and stem cell activity of resident progenitor/notochordal cells (increased number of CD24 positive cells). We are confident that the DWJ-based formulations proposed here can provide adequate stimuli to the cells present in the degenerated IVD to restart the anabolic machinery.

KEYWORDS

Decellularization, Wharton's Jelly, multifunctional hydrogels, Intervertebral disc cells

1. INTRODUCTION

The intervertebral disc (IVD) is the principal joint between two vertebrae in the spine. Not infrequently, its fibrocartilaginous structure can undergo degeneration due to various factors including bad lifestyles, aging, trauma, mechanical stress or genetic factors [1-2]. In many cases this causes severe spinal disorders that can significantly affect the individual's quality of life, leading to different forms of disability and a socioeconomic burden [3]. It goes without saying that the IVD degeneration (IDD), is a very complex phenomenon and to date there are many open questions. Specifically, two main aspects are actively debated, the first concerns the lack of adequate preclinical experimental models [4], the second the difficulty of developing satisfactory tissue engineering approaches due to the "harsh" environment that characterizes the degenerated IVD tissue [5-6]. It is therefore realistic to state that the various regenerative approaches prosed so far have led to very limited successes.

Numerous scientists investigating the degenerative mechanisms, agree in attributing the loss of integrity of the extracellular matrix (ECM) as a main cause of the onset of IDD [7]. The degeneration occurs when IVD cells lose their function, senescent cell clusters are formed and an inflammation process is firstly triggered and later maintained, impairing self-repair mechanisms; finally, the inflammatory process causes a strong anabolism/catabolism imbalance [8]. Strategies aimed to restore key signalling factors in the cellular dialogue or to give an adequate stimulus to the resident cells to restart the anabolic machinery, appear, therefore very promising [9-10].

In the current framework, the idea, at the base of the current article, is to make an attempt to ameliorate the functionality of the IVD cells embedded in a degenerated disc environment, by exploiting the properties of a specific ECM with high potential in regenerative medicine, namely the decellularized matrix obtained from the umbilical cord Wharton's jelly (DWJ) [11,12]. It is indeed well known that DWJ possesses several properties well suitable for tissue repair/engineering approaches, including biomechanical, immunomodulatory, antibacterial and biocompatibility features [13].

The human Wharton's jelly, in the last few years, has indeed received an increasing attention due to its potential for regenerative medicine applications as "natural constituent" to produce biomimetic scaffolds [14]. Interestingly, the Wharton's jelly mucoid connective tissue has a composition very similar to that of IVD extracellular matrix [15,16]. Notably, Wharton's Jelly is rich in matrix components such as hyaluronic acid, various types of collagens and sulphated glycosaminoglycans;

in addition, growth factors (FGF, IGFBP 1, 2, 3, 4 and 6) are present, together with TGF-α, GH and PDGF-AA. Immunomodulatory cytokines (RANTES, IL-6R, and IL-16), pro-inflammatory cytokines (MCSFR, MIP-1a), anti-inflammatory cytokines (TNF-RI, TNF-RII, and IL-1RA), homeostatic cytokines (TIMP-1 and TIMP-2), cytokines associated with wound healing and regenerative properties (ICAM-1, G-CSF, GDF-15, MCP-1, GDNF), and extracellular vesicles, are also present [17-21].

In consideration of the exceptionally rich and favourable composition, Wharton's Jelly, could be employed to produce several bioinspired scaffolds, characterized by the preservation of both the architecture and the biological components useful also to support the reparative processes in the IVD tissue [15,16].

In this respect, we had previously demonstrated that human degenerated IVD cells are able to restore at molecular level their normal phenotype when combined with DWJ [15]. This suggests that, if the decellularization process is well designed and controlled, the obtained ECM retains the architecture of the natural cell environment, together with the complex biomolecular and physical cues, giving support to the cell viability and functions.

Despite the enormous potential of decellularized ECMs, proved by many biological characterizations on which numerous evidence agree, questions remain open regarding the fabrication and usability of decellularized ECM-based scaffolds [21-24]. A biomaterial-based device needs in fact to possess several requirements to be clinically suitable. Just to mention a few, it requires to be safe, usable, mechanically sound and biologically tuned for the specific injection/implantation site [25].

To address this issue, it is therefore necessary to design and produce scaffolds with a tailored architecture and mechanical properties closer to that of IVD, without losing the ability to support cell proliferation, differentiation, synthesis and remodelling of the ECM and to restore the healthy microenvironment of the IVD [26,27].

In this respect, the present study, describes the preparation and characterization of DWJ based multifunctional hydrogels, in form of 3D millicylinders (afterwards named and mentioned as Wharton's Jelly millicylinders, abbreviated to WJMs), composed of a mixture of alginate, gelatine and DWJ. Different aspects were considered, including, the setup of the decellularization protocol, the usability and conservation of the devices, and finally the ex-vivo biological evaluation using human IVD cells in different culture conditions.

2. Materials and Methods

2.1. IVD cells isolation

Human samples were collected after written informed consent provided by the participants and approval of the Ethics Committee of the University of Ferrara and S. Anna Hospital (protocol no. 160998). Specifically, IVD cells were isolated from human lumbar disc tissues of patients (n=15) undergoing surgical discectomy (see table 1). The mean age of the donors was 58 years (range, 26-81 years, 11 males and 4 females, Pfirrmann grade 2-5). Nucleus pulposus tissue from each sample was macroscopically dissected from the annulus fibrosus and was subjected to enzymatic digestion using 1 mg/ml type IV collagenase (Merck KGaA, MA, USA) for 5 h at 37˚C in DMEM High Glucose /Ham's F12 (Euroclone S.p.A., Milan, Italy). The digested cell suspension was filtered through a Falcon™ 70 µm Nylon Cell strainer (BD Biosciences, NJ, USA). Subsequently, the cells were centrifuged at 300 x g for 10 min at room temperature, the supernatant was discarded, the cells (P0) were resuspended in medium [DMEM/F12 containing 10 % foetal calf serum (FCS; Euroclone S.p.A.), 100 mg/ml streptomycin, 100 U/ml penicillin and 1% Glutamine, Euroclone S.p.A.] and seeded in polystyrene culture plates (Sarstedt, Nümbrecht, Germany) at a density of 10000 cells/cm^2. P0 cells were expanded by growing for a period not exceeding a week until subconfluent, detaching by trypsinization, and maintained in culture for more than two passages to obtain IVD cells that were used for later experiments. As already demonstrated after monolayer culture expansion, cells isolated from human lumbar IVD become de-differentiated, lose their chondrogenic-like phenotype resembling the degeneration process [28] and subcultured up to passage 3.

2.2. Wharton's jelly decellularization

Human umbilical cords (all from natural deliveries) were collected after mothers' understanding and written informed consent and approval of the Ethics Committee of the University of Ferrara and S. Anna Hospital (protocol no. 061199/AOUFe). Cords were processed within 4 h, rinsed several times with sterile phosphate-buffered saline (PBS 1X, Euroclone S.p.A.) and cut into pieces (3 cm in length). The obtained sections were then dissected, after a longitudinal cut, to remove the epithelium and to expose the underlying Wharton's jelly. The soft gel tissue was finely chopped in pieces to about 1 mm^3. The obtained pieces were treated by agitation immersion, with a detergent-enzymatic treatment (DET) [29]. Briefly, samples were washed 2 times in PBS 1X, thereafter subjected to three DET cycles, each of them composed of the following steps. Immersion is deionized water at 4 °C for

24 h, immersion in a 4 % sodium deoxycholate (Merck KGaA) aqueous solution at room temperature for 4 h and finally, immersion in a 2000 kU DNase-I (Merck KGaA) dispersion in 1 M NaCl at RT for 3 h. Thereafter the treated samples were mechanically homogenized after dispersion in 0.1% sodium deoxycholate (Merck KGaA) at room temperature (RT). A high-speed mechanical homogenizer (T25 Ultra-Turrax, IKA-Werke GmbH & Co, Staufen, Germany), with a 7.5 mm diameter working head at the speed of 10000 rpm was employed, setting 4 cycles of homogenization of 1 m each, pausing for 30 seconds between each pulse. A final pulse of 5 minutes was carried out. The obtained homogenized samples were stored at 4°C.

2.3. Production of multifunctional millicylinders (WJMs)

The alginate and gelatin dispersions in water were prepared as follows. The biopolymer dispersions were obtained dispersing the sodium alginate powder (IE-1105/500) (Inotech Biosystems Int, MD, USA) or the gelatin powder (PS 150 7 30, type A; Sanofi, Paris, France) in water, under gentle stirring with a mechanical stirrer equipped with a stainless steel three blade impeller (200 rpm), for 2 h, at 40°C. In order to eliminate any large particle, the biopolymer dispersions, immediately after preparation, have been purified by filtration. Filtration was carried out with membrane filters with decreasing porosity, from 5.0 up to 0.22 µm (Durapore membrane filters, Merck KGaA). Before the final use, three dispersions so far obtained were stored in a refrigerator at + 4 °C. For the final preparation of millicylinders, a further filtration with a syringe equipped with a 0.22 µm membrane disc filter, was performed under sterile laminar flow hood. The gelling solutions for alginate were constituted with barium chloride ($BaCl_2$) (Merck KGaA) in water at 1.5% (w/v). All the solutions were prepared by dissolving the crystalline powder, weighed on an analytical balance, in ultrapure water and stored at 4 °C. To produce the scaffolds used in *in vitro* and *ex vivo* conditions, the solutions were filtered with a syringe equipped with a 0.22 µm membrane disc filter under sterile conditions.

The millicylinders were prepared with different composition in term of alginate, gelatin and DWJ content (see samples composition and identification codes in Table 2). Irrespectively of their composition, the millicylinders were produced by mixing the appropriate amount of the dispersions pre-warmed at 37°C.

Millicylinder samples made by alginate/gelatin/WJ concentration were prepared pouring 100 µl of the mixture of biopolymers in empty a cylindrical PDMS master and allowed to gel for 2 h at -20°C Therefore, the 3x4 mm (height/diameter) millicylinders were gently peeled from the silicon master. The ionic gelation of the alginate portion of the polymeric mixture was accomplished by immersion

of the samples in a $BaCl_2$ solution (prepared as previously stated) for 30 m at 5°C. Finally, the ionically cross-linked millicylinders were freeze dried overnight, after congealing at -20°C.

2.4 Experimental set up

For each set of experiments (Figure 1), WJMs were previously positioned in the upper chamber of 24w Transwell™ (8 µm porosity permeable support, Corning, NY, USA) culture system. In the lower chamber, IVD cells ($25x10^3$), or M1 polarized macrophages ($1x10^5$) or IVD biopsies (300 mg) were cultured in standard condition (1ml/well). Scratch assay was performed on IVD cells cultured in WJM conditioned medium which was obtained from WJMs kept alone for 72 hours in DMEM High Glucose/F12 without FCS.

2.5. Cell viability and proliferation

The viability of IVD cells cultured in the presence of WJM was determined by a live/dead cell imaging protocol, as previously described [21]. After staining with propidium iodide and Calcein-AM, cells were imaged by a fluorescence microscope (Nikon, Optiphot-2, Nikon corporation, Japan) using the specific filter blocks. Dead cells were stained in red, whereas viable ones in green. Conversely, the proliferation rate of IVD cells cultured in the presence of WJMs was determined by the AlamarBlue™ assay (cat.no. DAL 1025, Thermo Fisher Scientific, MA, USA). Briefly, cells were cultured in the presence or absence of WJM up to 15 days. After different length of time, the ready-to-use resazurin-based solution was added to the cells. After 4 h of incubation, 200 µL of the cell medium was transferred to a 96-well plate, and then the visible light absorbance was determined, by a microplate absorbance reader (SunriseTM, Tecan, Switzerland), at 570 nm (resorufin reduced form) and 620 nm (resazurin oxidized form). Plotted values correspond to the difference in absorbance between the reduced and oxidized forms of AlamarBlue™.

2.6. Phalloidin staining

After 3 days of cell culturing, IVD cells were fixed with a 4% paraformaldehyde solution, permeabilized with 0.1% Triton X-100 solution ((Merck KGaA) and then incubated in the presence AlexaFluor 488-Phalloidin (1:500 dilution, cat. no. A12379; Thermo Fisher Scientific). Cells were then counterstained with DAPI (1:1000 dilution, cat. no. D9542, Merck KGaA). Fluorescence images were captured by a Zeiss LSM800 Confocal microscope (Carl Zeiss Meditec AG, Oberkochen, Germany).

2.7. Scratch assay

The scratch assay was performed as follows. IVD cells were seeded into 24-well plates and incubated with complete medium at 37°C in 5% CO_2 atmosphere. After 24 h of culturing, the formed monolayer a linear scrape was formed by a sterile sharp tip (500 μm in diameter). After debris removal by PBS washing, the cells were cultured in the presence of WJM conditioned medium (without FCS). Cells cultured in DMEM High glucose/F12 represented the control. After culturing the IVD cells for different length of time (up to 72 h), the scratches were imaged under an inverted microscope (Nikon Corporation, Tokyo, Japan). To determine the migration, cell images were analysed using "ImageJ" software, determining the closed area with respect to initial scratch size at time 0. An increase of the wound closure area (calculated as follows) indicates the migration of cells; wound closure (%) = (measurement at time 0 − measurement at time 72 h)/measurement at time 0 × 100.

2.8. Monocytes isolation and M1 polarization

Monocytes were isolated from human peripheral blood (PB) of healthy volunteers (n=4) after informed consent by using sequential density gradient centrifugations over Ficoll (Merck KGaA) solution. The monocytes were cultured in RPMI 1640 medium with 10% FCS (Euroclone S.p.A.) and 25 ng/ml of human MCSF (cat.no. 300-25, PeproTech, London, UK) to differentiate them into macrophages. After 5 days, the M1 polarization (CTR, control cells) was begun by changing to fresh medium supplemented with 100ng/ml IFNγ (cat.no. 300-02, Peprotech) and 100ng/ml lipopolysaccharide (LPS, cat.no. L6529, Merck KGaA). Macrophages were also exposed to WJMs placed above a 24w Transwell ™, 8 μm porosity, up to 72 h. Phenotypic analysis of M1 polarization was performed by flow cytometry. Cells were incubated with either PE conjugated anti-human CD80 (clone REA661, Miltenyi biotec, Germany) and FITC conjugated anti human CD86 (clone 233, BD Biosciences, USA) for 30 min in the dark. Labelled cells were analyzed using FACS CANTO II (BD Bioscience), compensated using antibody capture beads (BD Bioscience). Flow cytometry data was analyzed using FlowJo (version 10.8, Tree Star Inc.). The concentrations of TNFα and IL12 was simultaneously evaluated in the supernatants of M1 polarized macrophages in the absence (control) and after exposition to WJM using multiplex bead-based sandwich immunoassay kits (cat.no. 171B5026M, TNFα; cat.no. 171B5011M, IL12; BioRad Laboratories Inc., Segrate, Italy) following the manufacturer's instructions. Briefly, we added 50μL to each well of the diluted standards (fourfold dilution series), controls and samples in triplicate and added 50μL of coupled beads and the plate was incubated at room temperature for 30 m. The plate was then washed three times of 100 μL

wash buffer and incubated with 25 µL of detection antibodies for 30 m. Finally, the plate was washed three times and incubated with 50 µL of streptavidin-PE for 30 min and measured in a reader (Bio-Rad Laboratories Inc.).

2.9. Immunocytochemistry

Immunocytochemistry analysis was performed using the ImmPRESS kit (cat. no. MP-7500; Vector Laboratories, Inc., CA, USA). Cells were plated at a density of 10000 cells/cm^2 in 24-culture plates in the presence of WJMs to up 7 days. Cells were fixed in cold methanol at room temperature for 10 min and permeabilized with a 0.2% (v/v) Triton X-100 (Merck KGaA) in Tris-buffered saline (TBS) at room temperature for 10 min. Cells were treated with H_2O_2 3% (v/v) in TBS at room temperature for 10 m, thereafter in 2% normal horse serum (Vector Laboratories, Inc.) for 15 min at room temperature. After serum treatment, primary antibodies against SOX9 (1:500), TRPS1 (1:100), FOXO3a (1:1000), ACAN (1:200), COL2a1 (1:200) were added and incubated at 4°C overnight [SOX9, cat. no. sc-20095, aggrecan, ACAN; cat. no. sc-33695, Santa Cruz Biotech, Inc.; FOXO3a, cat. no. ab70315 and collagen type II α1 chain (COL2a1) cat. no. ab3092, Abcam, Cambridge, UK; anti-tricho-rhino-phalangeal syndrome type I protein, zinc finger protein (TRPS1) cat. no. 20003-1-AP, ProteinTech Group, Inc., IL, USA]. After exposure to the primary antibodies, cells were rinsed in 1X TBS and incubated for 30 min at room temperature with ImmPRESS-HRP Universal Polymer reagent (horse anti-mouse/rabbit IgG), The final stain with a substrate/chromogen mix (ImmPACT™ DAB, Vector Laboratories, Inc) was performed for 5 min at room temperature. After washing, cells were mounted in glycerol/PBS (9:1) and observed under a Nikon Eclipse 50i optical microscope (Nikon Corporation). Semi-quantitative image analysis of immunostained cells was performed using the ImageJ software as previously reported [29].

2.10. Human organ culture model

IVD disc tissues from 3 patients (Pfirrmann grade 4-5) were processed within 16 h, chopped in small pieces (0.1-0.3 cm^3) and rinsed in PBS 1X containing 1% penicillin–streptomycin. Based on the wet weight, the tissues were placed in 24-wells plate (basal medium, see above) and divided equally (300 mg each) between control (untreated) and A075W3 group (in the presence of A075W3 millicylinder). After 7 days tissues were subjected to mild digestion with type IV collagenase (1 mg/mL) as already reported. Percentages of CD24 positive isolated cells were evaluated by flow cytometry. Briefly IVD cells were incubated in binding buffer (PBS 1X/2 mM EDTA/0.5% BSA) with PE conjugated anti-

human CD24 (clone REA832, Miltenyi biotec, Germany) for 30 m, 4°C, in the dark. Labelled cells were analysed using FACS CANTO II (BD Bioscience), compensated using antibody capture beads (BD Bioscience). Flow cytometry data was analysed using FlowJo (version 10.8, Tree Star Inc.). Furthermore, a tissue sample from each group was also fixed in 4% PFA (paraformaldehyde, Merck KGaA) and used for histochemical analysis.

2.11. Immunohistochemical analysis

IVD tissue samples after incubation with A075W3 millicylinders were rinsed with PBS1X , fixed in 4 % PFA for 24 h at 4 °C, embedded in paraffin and cross-sectioned (5-µm thick). For histological evaluation non-consecutive sections were immunoassayed with FOXO3a (cat. no. ab70315, 1:100 dilution; Abcam) TRPS1 (#20003-1-AP; 1:100 dilution; Abcam) and SOD-2 (cat. no. sc-133134; 1:100 dilution; Santa Cruz Biotech). Immunohistochemical sections were deparaffinized, rehydrated, and heated in sodium citrate (pH 6) for antigen retrieval. Slides were then processed with 3 % H_2O_2 in PBS for 5 min and with blocking solution (PBS 1X /1% BSA/10% FCS) for 30 min at room temperature. Then the slides were incubated over night with the primary antibody at 4 °C, followed by treatment with Vecstain ABC reagent (Vector Laboratories, Inc) for 30 min. The reactions were developed using DAB solution (Vector Laboratories, Inc), the sections were counterstained with haematoxylin and mounted in glycerol. The staining was quantified by a computerised video camera-based image analysis system (NIH, USA ImageJ software, public domain available at: http://rsb.info.nih.gov/nih-image/) under brightfield microscopy (NikonEclipse 50i; Nikon Corporation), as reported above. For the analysis of sections, positive cells in the area were counted and protein levels expressed as % of positive nuclei (ten fields per replicate, 5 sections per sample).

2.12. Statistical analysis

Data are reported as mean value ± standard deviation (SD). Unpaired Student's t-test was used for direct comparisons; multiple groups were compared by using one-way ANOVA, followed by Tukey's HSD post-hoc test. All statistical analyses were performed using Prism 6 software (GraphPad Software). P-values less than 0.05 were considered significant.

Table 1. Human IVD samples clinical informations

Donor	*IVD level*	*Age*	*Sex*	*Symptoms*	*Duration of symptoms prior to surgery*	*Pfirrmann grade*
#1	L4L5	62	female	radiculopathy: pain and palsy, neurogenic claudication	5 months	IV
#2	L4L5	49	male	radiculopathy: palsy	6 months	IV
#3	L4L5	57	male	radiculopathy: pain and palsy	2 months	IV
#4	L4L5	64	male	radiculopathy: pain	2 months	IV
#5	L4L5	46	male	radiculopathy: pain and palsy	1 month	III
#6	L4L5	80	male	radiculopathy: pain and palsy	48 months	IV
#7	L3L4	81	female	radiculopathy: pain	1 month	II
#8	L4L5	67	male	back pain and claudicatio	3 months	V
#9	L4L5	66	male	radiculopathy: pain	18 months	II
#10	L5S1	54	female	back pain and radiculopathy: pain and palsy	6 months	III
#11	L4L5	53	male	claudicatio	9 months	IV
#12	L4L5	45	male	radiculopathy: pain and palsy	7 months	III
#13	L5S1	26	female	radiculopathy: pain	12 months	IV
#14	L2L3	67	male	back pain and radiculopathy: pain and palsy	1 month	IV
#15	L4L5	64	male	radiculopathy: pain and palsy	4 months	IV

Table 2 Identification codes and composition of the biopolymers employed for the millicylinders (WJMs) preparation

Identification code	**Alginate (%, w/w)**	**Gelatin (%, w/w)**	**WJ (%, w/w)**
$A_{075}G_3$	0.75	3.00	n.p.
$A_{075}G_{15}W_{15}$	0.75	1.50	1.50
$A_{075}W_3$	0.75	n.p.	3.00
$A_{075}W_6$	0.75	n.p.	6.00
$A_{075}W_{15}$	0.75	n.p.	1.50

n.p. = not present

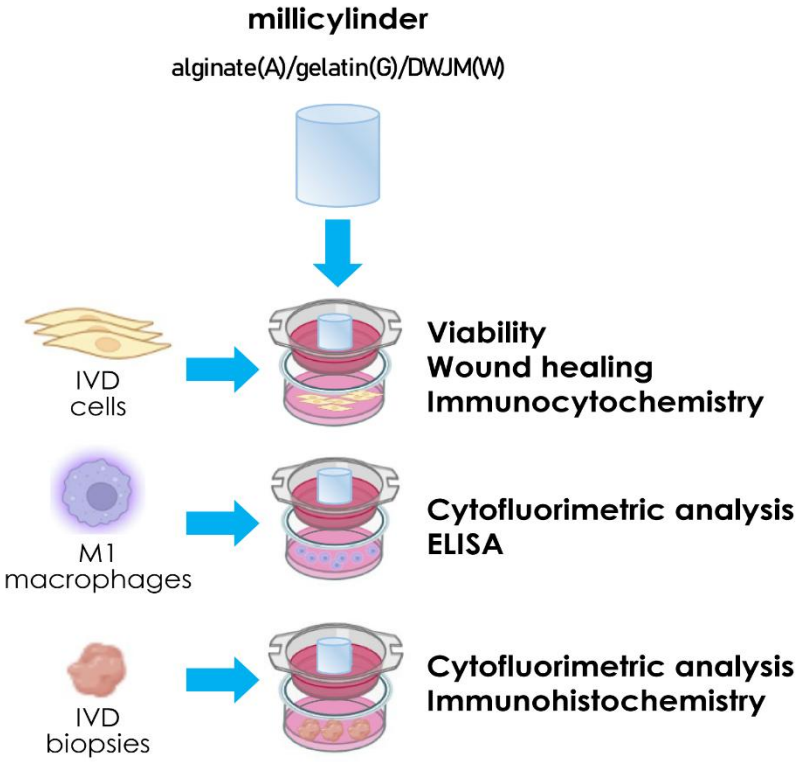
millicylinder
alginate(A)/gelatin(G)/DWJM(W)
IVD
cells
Viability
Wound healing
Immunocytochemistry
M1
macrophages
Cytofluorimetric analysis
ELISA
IVD
biopsies
Cytofluorimetric analysis
Immunohistochemistry

Figure 1

3. RESULTS and DISCUSSION

3.1. Production of WJMs: general considerations

Thanks to their high-water contents, soft consistency and controlled 3D environment, hydrogels have found numerous applications, in the medical and pharmaceutical fields [26, 31-34]. In this respect, it is important to underline that the great success of multifunctional hydrogels (i.e., especially those with natural constituents) for biomedical applications lays in the structural, biochemical and biomechanical similarity with the native ECM, displaying a rich ligand landscape able to influence cell behaviours [35, 36].

More specifically, one of the main goals of the present paper is to develop biomaterial-based scaffolds possessing an integrated number of properties. In this respect, we describe here newly designed millicylinders, basically formulated with the well-validated polymers alginate and gelatin, offering the possibility to modulate/adjust the mechanical properties of the final millicylinders by the combined action of two different gelling behaviour: the ionotropic properties of alginate and the thermotropic properties of gelatin. The possibility to interact with cells is added to the mechanical function provided by alginate/gelatin, through the use of decellularized Wharton's Jelly, a potential added value to the millicylinders (afterwards named and mentioned as WJMs) that represent the focus of our investigation.

In this approach, cell grown in the presence or on the surface of the millicylinders can benefit from the bioconstituents present in the DWJ, such as hyaluronate, proteoglycans, peptide growth factors and lipid molecules that can improve cell viability and/or functions [17].

Moreover, multifunctional hydrogels containing a large proportion of inner water allow free diffusion of molecules and supramolecular aggregates [37] (e.g., the vesicles present in the DWJ), while the scaffolding polymers confer specific viscoelastic properties that are not found in either a pure solid or a pure liquid material. Moreover, hydrogels can be fabricated into different shapes and sizes from nano-scale particles to centimetres long sheets and 3D solids [38].

Finally, it is worth to mention that the presence of alginate offers an additional "function": the alginate in fact possesses immunobarrier properties [39], offering an immunoprotective function that allows the implantation of the graft and the survival without treatment of the recipients with immunosuppressive protocols.

With respect to the present investigation, the production of WJMs was accomplished by a replica molding approach, using PDMS molds (see Figure 2 panel A, B), in which the various biopolymer

mixtures were poured. For the complete biomaterial composition of the produced WJMs and they respective identification codes (later mentioned in the Result section and Figure captions) see Table 1. The developed protocol, based on a freezing step, leads to the consolidation of the entire polymeric dispersion mixture (by freezing the samples at -20°C), followed by an ionic gelation step (i.e, of the alginate component), which allows the consolidation of the obtained millicylinders (WJMs) at room temperature. After gelation of the freshly prepared WJMs (see Figure 2, panels C-E), the samples were subjected to a freeze-drying process, resulting in a porous, stable, easily storable and suitable matrix for ex-vivo experiments.

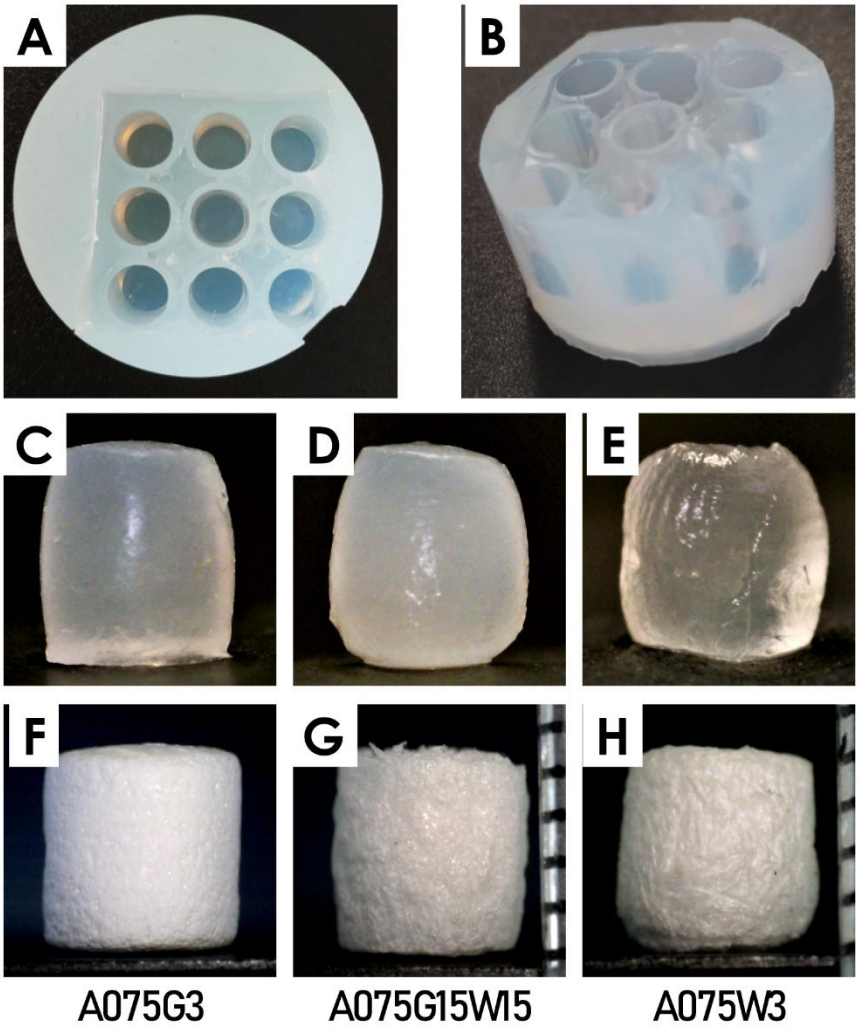

Figure 2

3.2. Effect of WJMs on viability, proliferation and wound closure ability of IVD cells

The experiments to evaluate the biological properties of the three different formulations were conceived by monitoring the cellular response to the soluble factors which were collectively released

into the culture medium (see the schematic overview of the experimental plan reported in Figure 1). For this purpose, human IVD cells isolated from degenerated disc tissue of patients undergoing spinal surgery and expanded up to passage three (P3) cells were used. As previously described, expansion in culture causes cells to dedifferentiate and lose their chondrogenic-like phenotype resembling the degeneration process [29]. The use human IVD primary cells represent an added value with regards to obtaining data that are in certain aspects more informative than the use of an animal model; however, the difficulty of isolation from surgical biopsies and the scarcity of cells obtainable from a tissue like this with low cellularity inevitably limits the number of experiments that can be performed. For these reasons, we were able to combine cells with a limited number of WJMs. Specifically, in a first step, the potential stimuli from three WJMs, A075G3, A075G15W15 and A075W3, were evaluated on viability, proliferation and wound closure ability of the cells (Figure 3 and Figure 4). Staining with Calcein AM/propidium iodide and FITC-conjugated phalloidin (Figure 3) showed that cells were viable after 72 h in culture, with no appreciable changes in cell morphology and cytoskeletal organization. The evaluation of proliferation performed with Alamarblue™ showed that cells receive some proliferative stimulus from all three formulations, especially from A075W3 and even more from A075G15W15 (Figure 3). Scratch assay was then performed on injured adherent IVD cell layers maintained over the next 72 hours in the culture medium in which the WJMs had previously been kept for 48 hours. Notably, as reported in Figure 4, conditioned medium from A075W3 induced a 17.89 ±3.22 wound closure that is significantly higher than that produced by the conditioned media from A075G3 and A075G15W15, or by control medium. It is important to underline that the recovery of a certain migratory capacity by the IVD cells is very critical for the regeneration of the disc, since this activity
is usually lost in the degenerated IVD microenvironment [40].

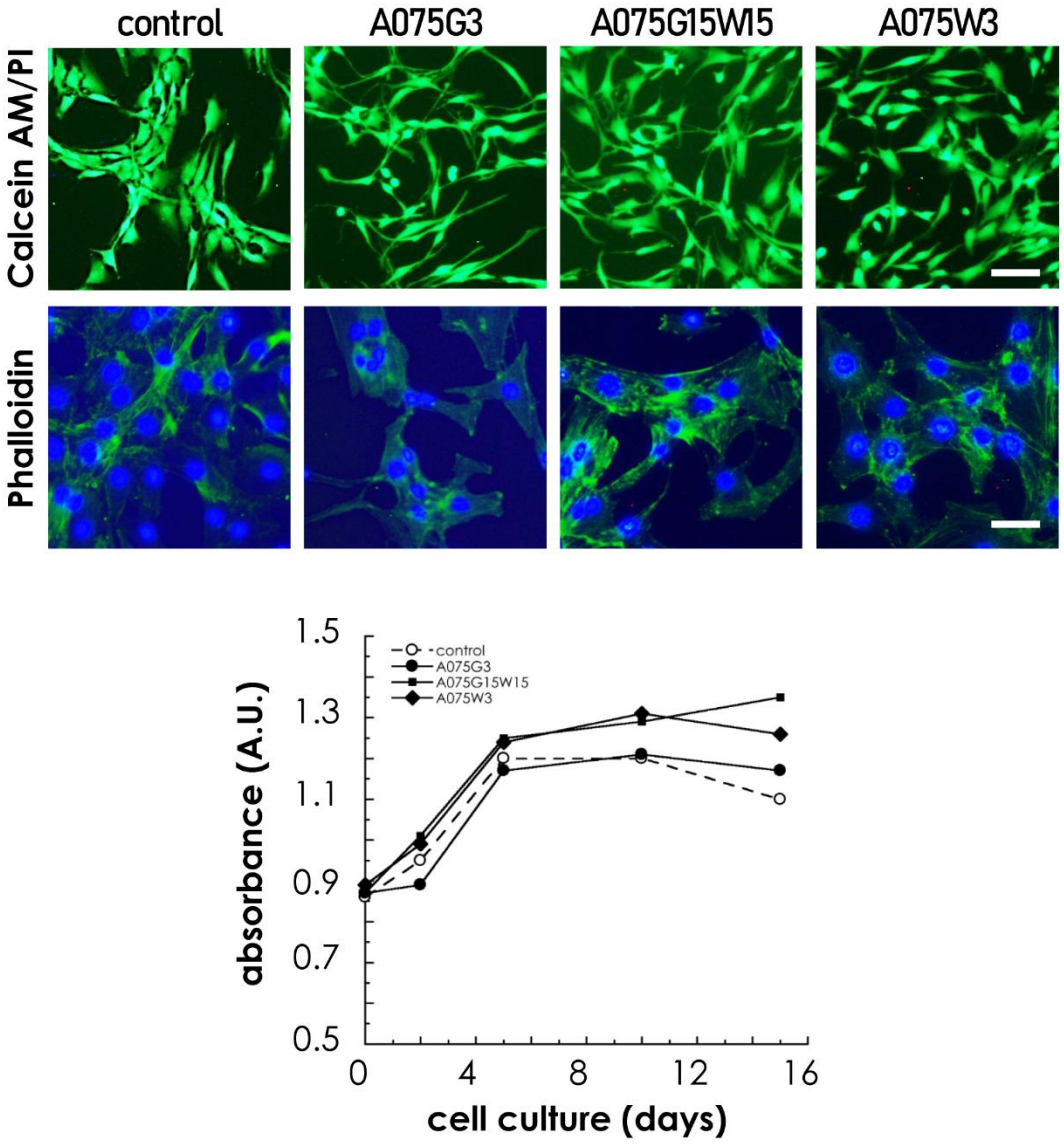
control
A075G3
A075G15W15
A075W3
Calcein AM/PI
Phalloidin
absorbance (A.U.)
cell culture (days)
control
A075G3
A075G15W15
A075W3
1.5
1.3
1.1
0.9
0.7
0.5
0
4
8
12
16

Figure 3

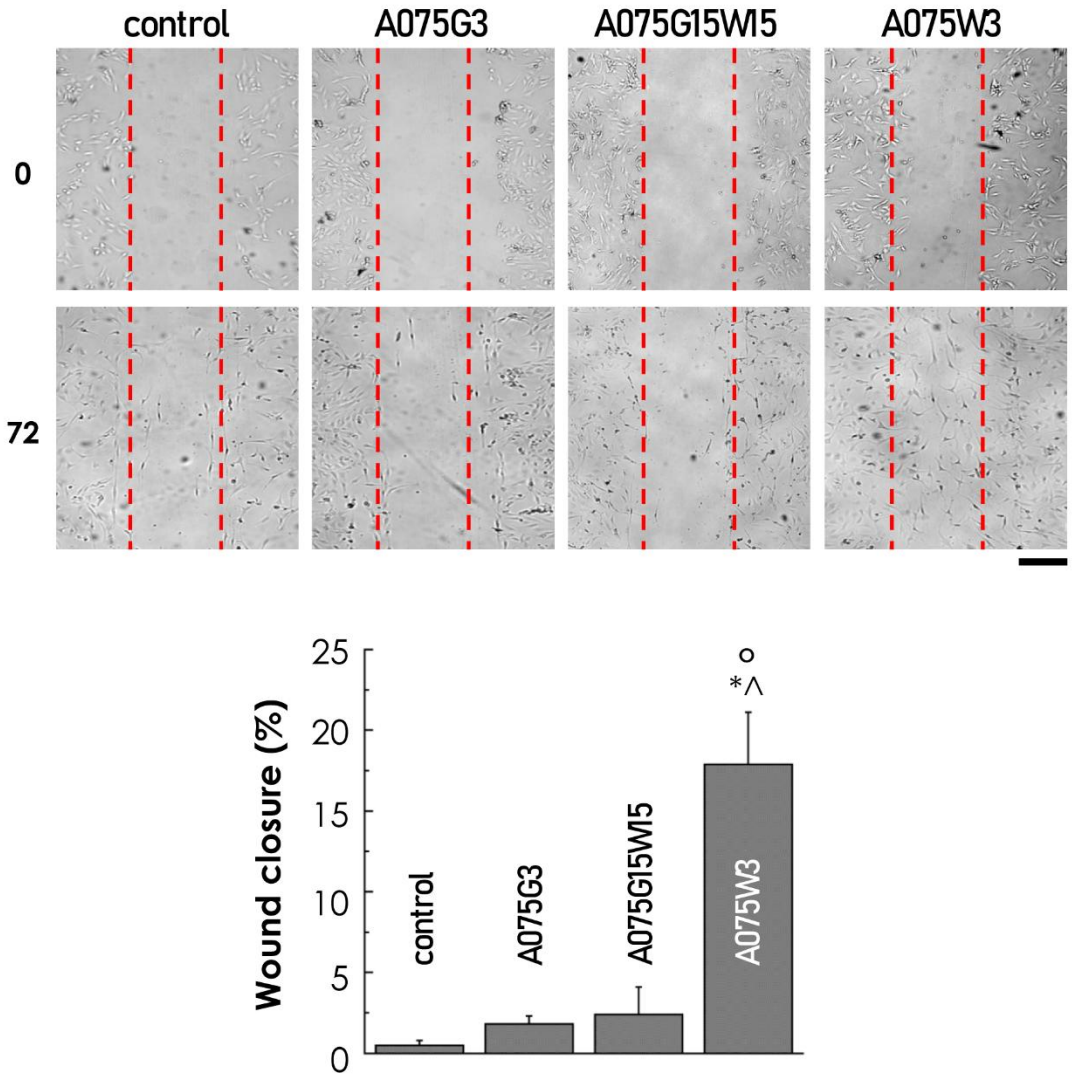

Figure 4

3.3. Effect of WJMs on M1 polarized human macrophages

The anti-inflammatory potential of the WJMs was investigated in a preliminary study aimed at evaluating the response of macrophages in culture. For this purpose, human monocytes were differentiated to macrophages through the addition of MCSF, polarized to pro-inflammatory M1

phenotype with LPS and IFNγ (as detailed in the Material and Methods section), and subjected for 48 h to the stimuli from the three WJMs, A075G3, A075G15W15 and A075W3. The expression level of two pro-inflammatory surface markers (CD80 and CD86), and the secretion of two pro-inflammatory cytokines (TNFα and IL-12) was evaluated by flow cytometry and ELISA immunoassay, respectively. As shown in Figure 5, A075W3 is the multifunctional millicylinder that, among those analyzed, is the particularly effective one ~~more than the others, is effective~~ in downregulating pro-inflammatory phenotypes in macrophages. Among the evaluated markers, the most significant reduction of expression concerns the CD80. The decrease in CD86 expression and in TNFα secretion is appreciable but not significant, while the modulation of IL-12 is unaffected.

These data suggest that the combination with alginate and gelatin still allows the anti-inflammatory properties of the DWJ to be maintained at a substantial level [17]. Obviously, future in vivo experiments on animal models will be needed to confirm this aspect.

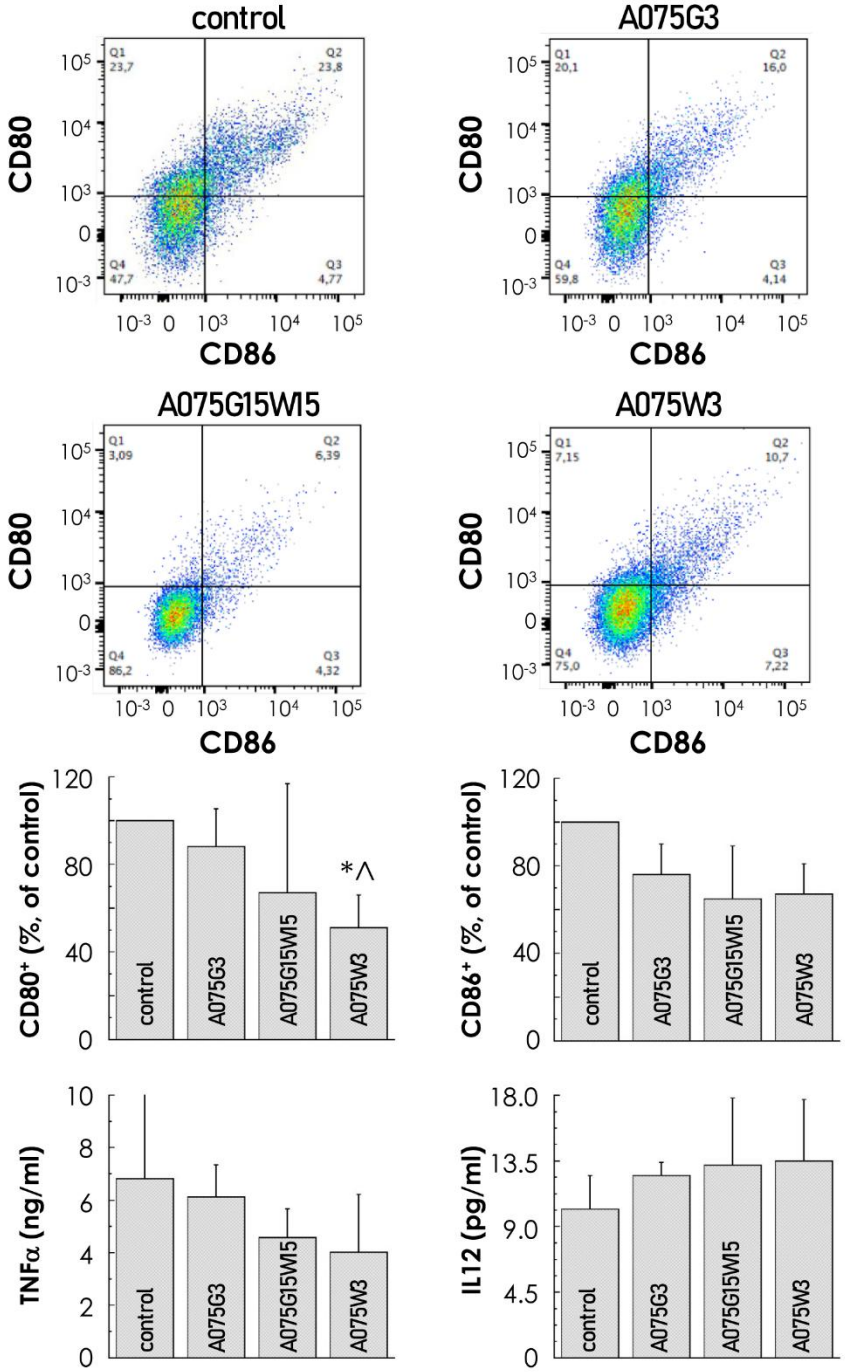

Figure 5

3.4. Effect of WJMs on IVD cell phenotype

The differentiation potential of the WJMs was investigated by evaluating the expression of ECM components (type II collagen α1 chain and Aggrecan) and pro-discogenic transcription factors (SOX9,

TRPS1 and FOXO3a) [41] in IVD cells after 7 days in culture. This analysis was the one which, more than others, demonstrated how relevant the presence of DWJ in the WJMs is. Except for TRPS1 whose expression remained always unchanged, soluble factors released by A075G15W15 and even more by A075W3, but not by A075G3, significantly increased the expression of all other markers, as revealed by immunocytochemical analysis (Figure 6). Therefore, the collected evidence suggested that A075W3 was the most promising formulation, considering the efficacy on reverting IVD degenerated phenotype. To further investigate the biological effect of A075W3 and establish a possible dose-response relationship between the presence of DWJ and the expression levels of the analyzed markers, WJMs with the same percentage of alginate but with different percentages of DWJ were produced and compared. A preliminary analysis was performed on WJMs with DWJ 1.5% (w/v) and DWJ 6% (w/v), designated A075W15 and A075W6 respectively (Table 2). After 7 days of culture, immunocytochemical analysis revealed that the expression levels of Aggrecan were not affected by the percentage of DWJ, while the expression level of the other proteins, in particular SOX9, FOXO3a and type II collagen α1 chain, continued to be positively modulated by A075W3 (Figure 7). While these data need to be validated with other experiments, yet these preliminary data suggest that there is a concentration range of DWJ around which the WJMs performs its optimal effect, and that an improvement in the IVD phenotype is not proportional to the increase in the amount of DWJ in the millicylinder.

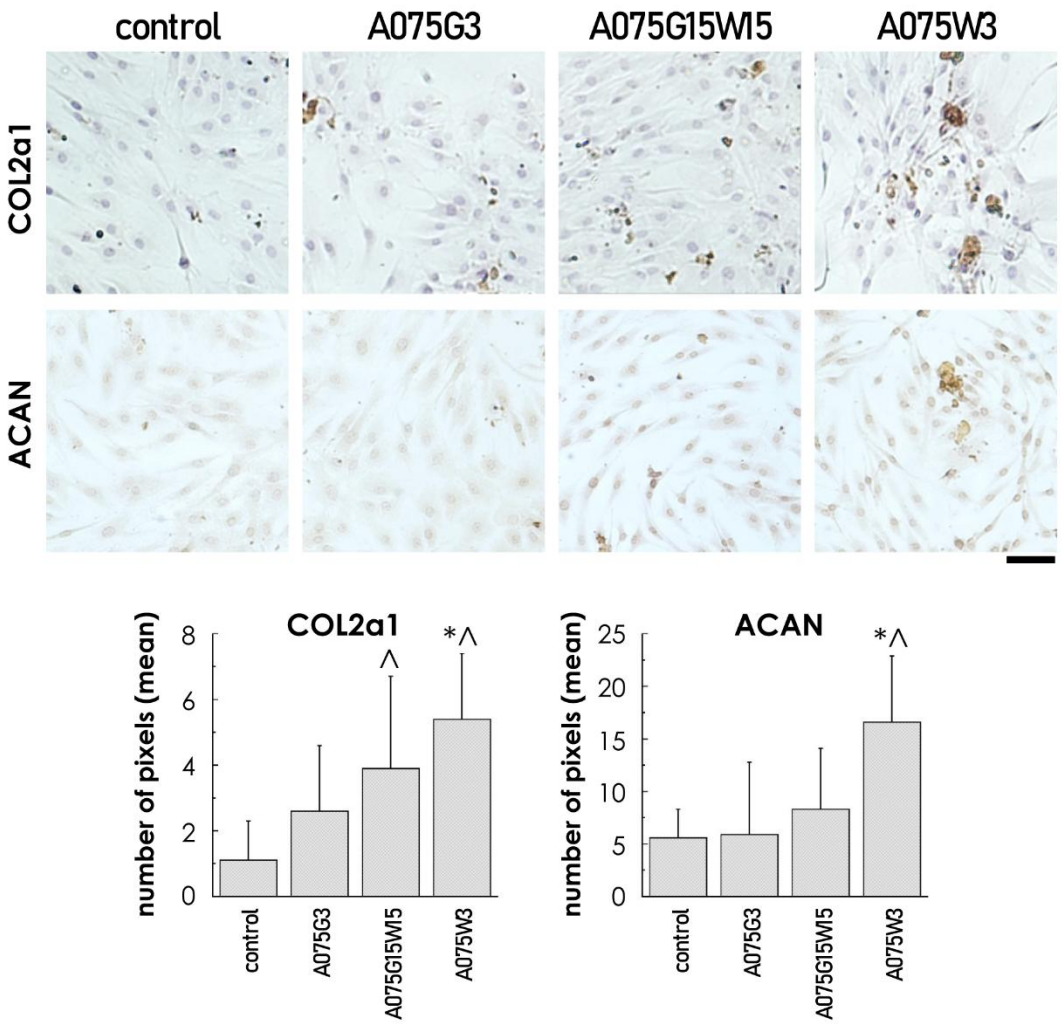
control
A075G3
A075G15W15
A075W3
COL2a1
ACAN
COL2a1
number of pixels (mean)
0
2
4
6
8
*^
^
control
A075G3
A075G15W15
A075W3
ACAN
number of pixels (mean)
0
5
10
15
20
25
*^
control
A075G3
A075G15W15
A075W3

Figure 6A

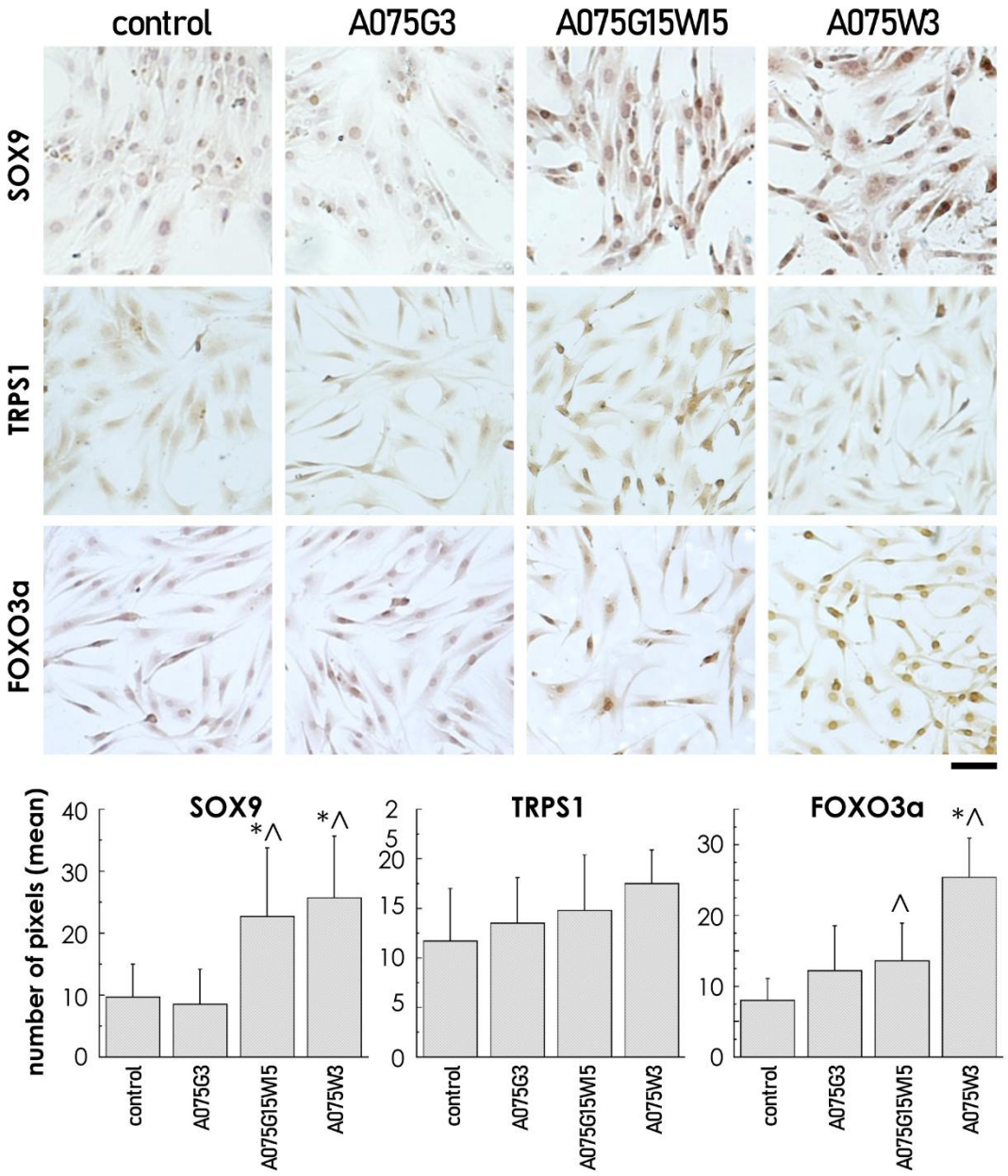
control
A075G3
A075G15W15
A075W3
SOX9
TRPS1
FOXO3a
SOX9
TRPS1
FOXO3a
number of pixels (mean)
*^
*^
^
control
A075G3
A075G15W15
A075W3

Figure 6B

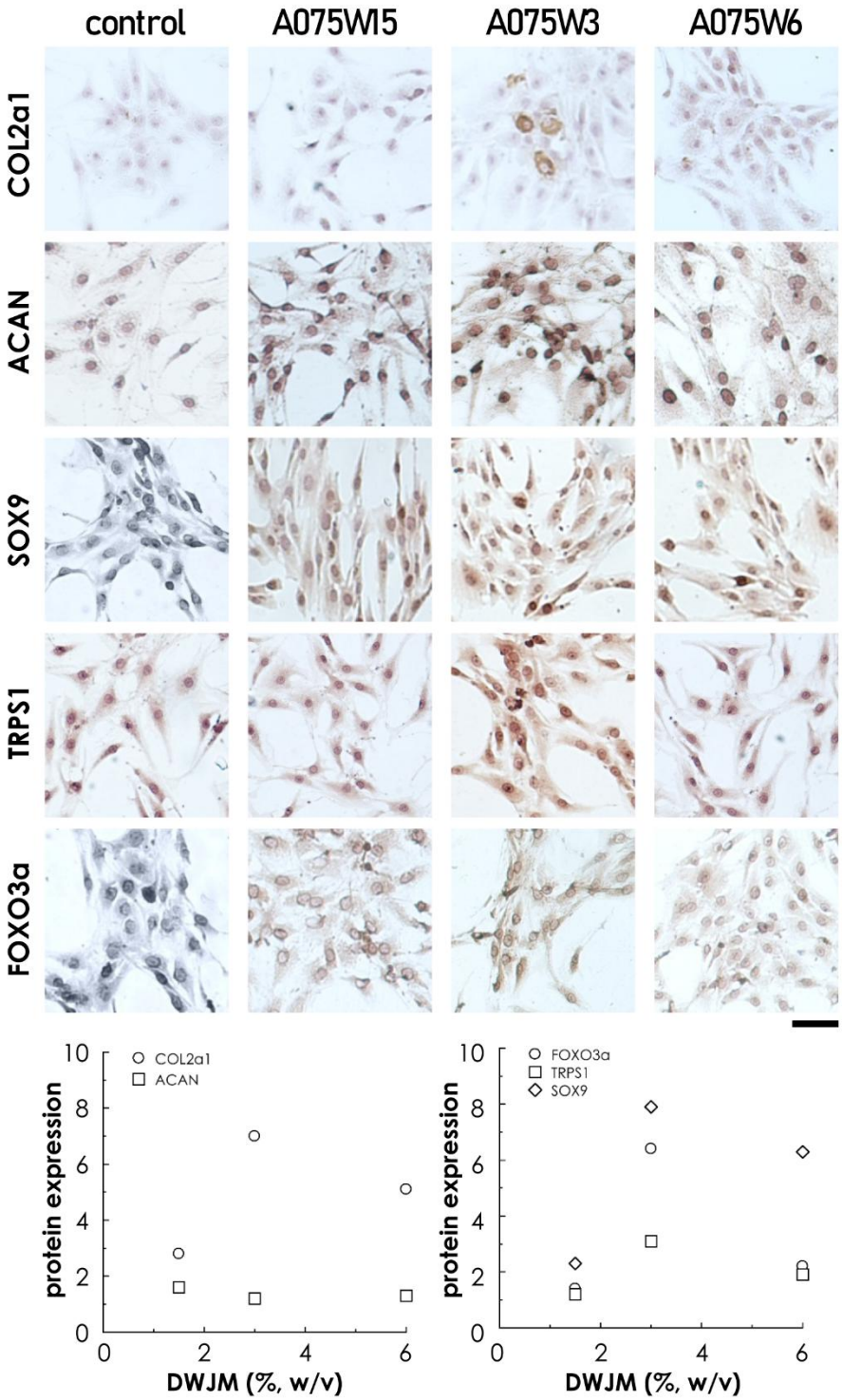

Figure 7

3.5. Effect of A075W3 multifunctional millicylinder on organ IVD culture model

As a final analysis, attention was focused on A075W3, the WJM which, according to the biological evaluations performed, proved to be more effective than the other. The potential of soluble factors released by it was evaluated on IVD biopsy fragments placed in culture for 7 days as organ IVD culture

model [41]. For this purpose, data collected from three different patients were evaluated separately. After 7 days in culture, the IVD fragments were subjected to immunohistochemical analysis for pro-discogenic transcription factors FOXO3a and TRPS1 as well as for the superoxide dismutase SOD2, a mitochondrial enzyme related to the antioxidant and redox signaling [43], and CD24 antigen [44]. CD24 is associated with the phenotype of notochordal cells, the embryonic precursors of all cells found in the nucleus pulposus (NP) of mature IVD and in part retained in the adult NP [45, 46]. Notably, the loss of notochord cells has been correlated with the pathogenesis of disc degeneration [47], conversely it has been described the protective effect of CD24-positive IVD cells against disc degeneration [44]. The data reported in Figure 8 suggest that the released factors are perceived by the IVD tissue fragments that respond positively to the stimuli with a tendency to raise the levels of the analysed markers with only two exceptions concerning CD24 and SOD2 in sample #6. Interestingly, the presence of A075W3 multifunctional millicylinder was particularly effective in the two samples (#14 and #15) with appreciable basal levels of CD24 positive cells. The approach proposed here presents some limitations represented by the few samples examined, a single exposure time and a small number of functional markers analysed. However, it should be considered a proof of concept for the development of a human experimental model useful for testing the efficacy of therapies designed to reactivate the endogenous regenerative properties of the IVD microenvironment.

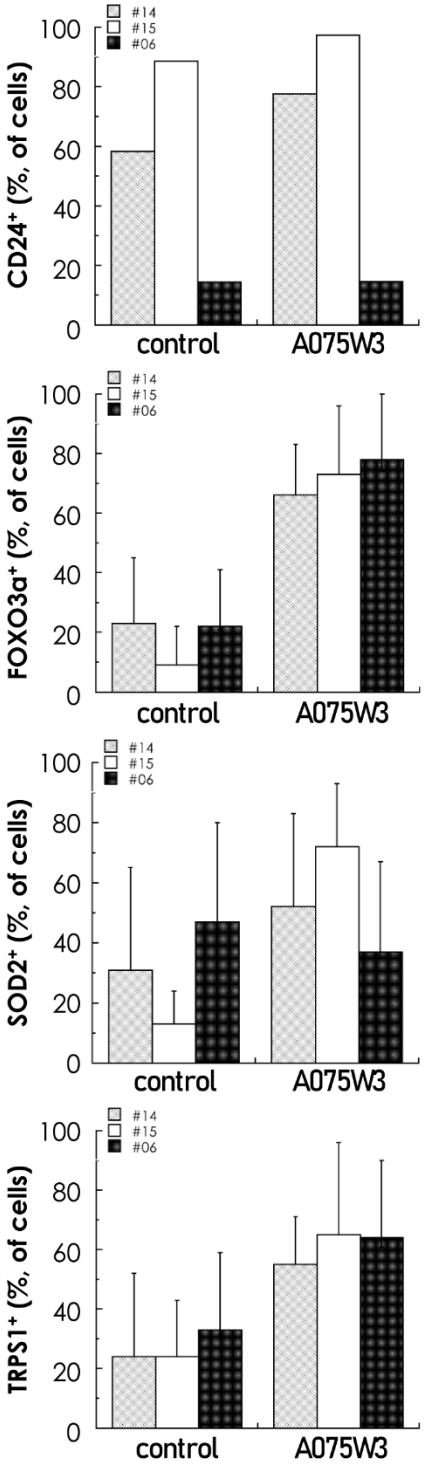
#14
#15
#06
CD24+ (%, of cells)
FOXO3a+ (%, of cells)
SOD2+ (%, of cells)
TRPS1+ (%, of cells)
0
20
40
60
80
100
control
A075W3

Figure 8A

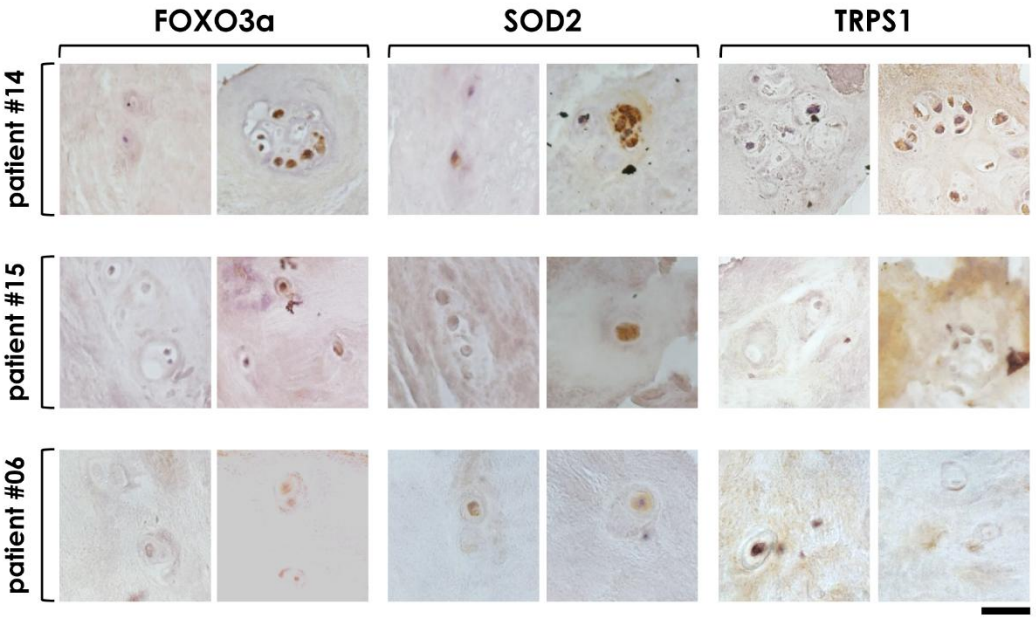

Figure 8B

4. CONCLUSIONS

The current investigation describes a new approach for the production of multifunctional millicylinders as tools for the treatment of intervertebral disc degeneration (IDD). Notably, the search of innovative approaches for IDD treatment is particularly active as proved by a number of published papers. In this respect,

intra-IVD injection of mesenchymal stromal cells (MSC) [49], MSC-derived extracellular vesicles (MSC-EVs) [50] and growth factors such IGF-1, BMP-7, BMP-2 and BMP-4 [51-52], have been identified not always effective in delaying or even reversing IDD. Nevertheless, the employment of ECM-based hydrogels [28], the combination alginate/hyaluronic acid in injectable scaffolds [31] often associated with anti-inflammatory biomolecules clearly exhibiting chemicals and physical properties, resembling IVD physiological environment and opening new opportunities for treatment. Therefore, considering the currently available data on the production of biomaterials for IDD, the results contained in the current manuscript suggest that the WJMs represent very promising tools for future clinical applications. Particularly interesting is indeed the possibility to adjust the composition of the millicylinders, fitting to the specific patient's needs. Indeed, it is worth mentioning that the composition and the mechanical properties of ECM of IVD varies depending on the anatomical site within the spine [6]. Consequently, it is important to develop biomaterials tailored to match the unique signature of ECM associated to the different IDD subtypes (disc fibrosis, disc calcification and disc herniations) [48]. Thus, the here proposed millicylinders could appropriately challenge the current needing of precise tissue engineering approach based on bioinspired scaffolds with tuneable biological properties.

Our findings suggest that the WJMs we obtained are very promising for future clinical application as it can be suitably modified, can become multifunctional and therefore tailored to the patient's needs. These biomaterials represent an important perspective for IVD regeneration can effectively replace the function of the natural disk in humans. Indeed, it is worth mentioning that in IVD, ECM profile varies depending on anatomical position and mechanical properties of each region within the spine [6]. Consequently, the ECM exhibits a unique signature in each of degenerative phenotypes that characterize the different IDD subtypes (disc fibrosis, disc calcification and disc herniations) [48]. Thus, the greatest challenge currently lies in developing a precision tissue engineering approach based on bioinspired scaffolds with tuneable biological properties such as the WJMs proposed here.

Data Availability

The data that support the findings of this study are available from the corresponding author upon reasonable request.

Conflicts of Interest

The authors declare that there are no conflicts of interest.

Authors' Contributions

L. P carried out in vitro cell work, analysis of data, manuscript review and editing; A.C carried out decellularization of Wharton's jelly, imaging and data processing; M.P.N carried out immunohistochemical analysis; B.D carried out FACS experiments; G.L performed citokynes quantification; P. G provided umbilical cords and participated in the manuscript review; R. P developed conceptualization, supervision, funding acquisition, manuscript review, and editing; C.N developed WJMs design and fabrication, developed conceptualization, study design, supervision and writing of the original draft and editing.

Funding Statement

This work was supported by FAR 2022 grants (University of Ferrara) to RP, CN and LP.

Acknowledgments

The authors thank Prof. Pasquale De Bonis and Dr. Chiara Angelini (Department of Neurosurgery, University Hospital of Ferrara) for patient recruitments; Dr. Francesco Nicoli (Chemical, Pharmaceutical and Agricultural Sciences, University of Ferrara) and Dr. Cristina Manferdini (IRCCS Istituto Ortopedico Rizzoli, Bologna, Italy) for technical support.

REFERENCES

Alexander A, Green WS. Total hip replacements: A second look. *J. Soc. Biomater.* 1989; *45*: 345–366.

[1] A.D. Diwan and Melrose J., "Intervertebral disc degeneration and how it leads to low back pain," *JOR Spine*, vol. 6, no.1, e1231, 2022. doi: 10.1002/jsp2.1231.

[2] Kang L, Zhang H, Jia C, Zhang R, Shen C. Epigenetic modifications of inflammation in intervertebral disc degeneration. Ageing Res Rev. 2023 Jun;87:101902. doi: 10.1016/j.arr.2023.101902. Epub 2023 Mar 4. PMID: 36871778.

[3] Yap ZL, Summers SJ, Grant AR, Moseley GL, Karran EL. The role of the social determinants of health in outcomes of surgery for low back pain: a systematic review and narrative synthesis. Spine J. 2022 May;22(5):793-809. doi: 10.1016/j.spinee.2021.11.013. Epub 2021 Nov 27. PMID: 34848343.

[4] Mohd Isa IL, Mokhtar SA, Abbah SA, Fauzi MB, Devitt A, Pandit A. Intervertebral Disc Degeneration: Biomaterials and Tissue Engineering Strategies toward Precision Medicine. Adv Healthc Mater. 2022 Jul;11(13):e2102530. doi: 10.1002/adhm.202102530. Epub 2022 May 4. PMID: 35373924.

[5] Tavakoli J, Diwan AD, Tipper JL. Advanced Strategies for the Regeneration of Lumbar Disc Annulus Fibrosus. Int J Mol Sci. 2020 Jul 10;21(14):4889. doi: 10.3390/ijms21144889. PMID: 32664453; PMCID: PMC7402314.

[6] Kibble, M.J.; Domingos, M.; Hoyland, J.A.; Richardson, S.M. Importance of Matrix Cues on Intervertebral Disc Development, Degeneration, and Regeneration. Int. J. Mol. Sci. 2022, 23, 6915. https://doi.org/10.3390/ijms23136915

[7] van Uden S, Silva-Correia J, Oliveira JM, Reis RL. Current strategies for treatment of intervertebral disc degeneration: substitution and regeneration possibilities. Biomater Res. 2017 Oct 23;21:22. doi: 10.1186/s40824-017-0106-6. PMID: 29085662; PMCID: PMC5651638.

[8] Silwal P, Nguyen-Thai AM, Mohammad HA, Wang Y, Robbins PD, Lee JY, Vo NV. Cellular Senescence in Intervertebral Disc Aging and Degeneration: Molecular Mechanisms and Potential Therapeutic Opportunities. Biomolecules. 2023 Apr 18;13(4):686. doi: 10.3390/biom13040686. PMID: 37189433; PMCID: PMC10135543.

[9] Wangler S, Peroglio M, Menzel U, Benneker LM, Haglund L, Sakai D, Alini M, Grad S. Mesenchymal Stem Cell Homing Into Intervertebral Discs Enhances the Tie2-positive Progenitor Cell Population, Prevents Cell Death, and Induces a Proliferative Response. Spine (Phila Pa 1976). 2019 Dec 1;44(23):1613-1622. doi: 10.1097/BRS.0000000000003150. PMID: 31730570; PMCID: PMC6867676.

[10] Singh S, Patel AA, Singh JR. Intervertebral Disc Degeneration: The Role and Evidence for Non-Stem-Cell-Based Regenerative Therapies. Int J Spine Surg. 2021 Apr;15(s1):54-67. doi: 10.14444/8055. Epub 2021 Apr 19. PMID: 34376496; PMCID: PMC8092937.

[11] Azarbarz N, Khorsandi L, Nejaddehbashi F, Neisi N, Nejad DB. Decellularized Wharton's jelly scaffold enhances differentiation of mesenchymal stem cells to insulin-secreting cells. Tissue Cell. 2022 Dec;79:101938. doi: 10.1016/j.tice.2022.101938. Epub 2022 Sep 16. PMID: 36152380.

[12] Muthuchamy M, Subramanian K, Padhiar C, Dhanraj AK, Desireddy S. Feasibility study on intact human umbilical cord Wharton's jelly as a scaffold for human autologous chondrocyte: In-vitro study. Int J Artif Organs. 2022 Nov;45(11):936-944. doi: 10.1177/03913988221118102. Epub 2022 Aug 18. PMID: 35982588.

[13] Dubus M, Scomazzon L, Chevrier J, Montanede A, Baldit A, Terryn C, Quilès F, Thomachot-Schneider C, Gangloff SC, Bouland N, Gindraux F, Rammal H, Mauprivez C, Kerdjoudj H. Decellularization of Wharton's Jelly Increases Its Bioactivity and Antibacterial Properties. Front Bioeng Biotechnol. 2022 Mar 11;10:828424. doi: 10.3389/fbioe.2022.828424. PMID: 35360386; PMCID: PMC8963334.

[14] Fayon A, Helle D, Francius G, Vincourt JB, Regnault V, Dumas D, Menu P, El Omar R. Characterization of an Innovative Biomaterial Derived From Human Wharton's Jelly as a New Promising Coating for Tissue Engineering Applications. Front Bioeng Biotechnol. 2022 Jun 13;10:884069. doi: 10.3389/fbioe.2022.884069. PMID: 35769101; PMCID: PMC9234273

[15] Penolazzi L, Pozzobon M, Bergamin LS, D'Agostino S, Francescato R, Bonaccorsi G, De Bonis P, Cavallo M, Lambertini E, Piva R. Extracellular Matrix From Decellularized Wharton's Jelly Improves the Behavior of Cells From Degenerated Intervertebral Disc. Front Bioeng Biotechnol. 2020 Mar 27;8:262. doi: 10.3389/fbioe.2020.00262. PMID: 32292779; PMCID: PMC7118204.

[16] Penolazzi L, Lambertini E, D'Agostino S, Pozzobon M, Notarangelo MP, Greco P, De Bonis P, Nastruzzi C, Piva R. Decellularized extracellular matrix-based scaffold and hypoxic priming: A promising combination to improve the phenotype of degenerate intervertebral disc cells. Life Sci. 2022 Jul 15;301:120623. doi: 10.1016/j.lfs.2022.120623. Epub 2022 May 7. PMID: 35537547.

[17] Gupta A, El-Amin SF 3rd, Levy HJ, Sze-Tu R, Ibim SE, Maffulli N. Umbilical cord-derived Wharton's jelly for regenerative medicine applications. J Orthop Surg Res. 2020 Feb 13;15(1):49. doi: 10.1186/s13018-020-1553-7. PMID: 32054483; PMCID: PMC7017504.

[18] Jadalannagari S, Converse G, McFall C, Buse E, Filla M, Villar MT, Artigues A, Mellot AJ, Wang J, Detamore MS, Hopkins RA, Aljitawi OS. Decellularized Wharton's Jelly from human umbilical cord as a novel 3D scaffolding material for tissue engineering applications. PLoS One. 2017 Feb 21;12(2):e0172098. doi: 10.1371/journal.pone.0172098. Erratum in: PLoS One. 2017 Mar 7;12 (3):e0173827. PMID: 28222169; PMCID: PMC531968

[19] Li D, Chiu G, Lipe B, Hopkins RA, Lillis J, Ashton JM, Paul S, Aljitawi OS. Decellularized Wharton jelly matrix: a biomimetic scaffold for ex vivo hematopoietic stem cell culture. Blood Adv. 2019 Apr 9;3(7):1011-1026. doi: 10.1182/bloodadvances.2018019315. PMID: 30940636; PMCID: PMC6457237.

[20] Xu, Y., Duan, L., Li, Y. Q., She, Y. L., Zhu, J. J., Zhou, G. D., Jiang, G. N., Yang, Y., Nanofibrillar Decellularized Wharton's Jelly Matrix for Segmental Tracheal Repair. Adv. Funct. Mater. 2020, 30, 1910067. https://doi.org/10.1002/adfm.201910067

[21] Penolazzi L., Tavanti E., Vecchiatini R., Lambertini E., Vesce F., Gambari R., et al. (2010). Encapsulation of mesenchymal stem cells from Wharton's jelly in alginate microbeads. Tissue Eng. C Methods 16 141–155. 10.1089/ten.TEC.2008.0582

[22] Zhe, M.; Wu, X.; Yu, P.; Xu, J.; Liu, M.; Yang, G.; Xiang, Z.; Xing, F.; Ritz, U. Recent Advances in Decellularized Extracellular Matrix-Based Bioinks for 3D Bioprinting in Tissue Engineering. Materials 2023, 16, 3197. https://doi.org/10.3390/ma16083197

[23] Giobbe GG, Crowley C, Luni C, Campinoti S, Khedr M, Kretzschmar K, De Santis MM, Zambaiti E, Michielin F, Meran L, Hu Q, van Son G, Urbani L, Manfredi A, Giomo M, Eaton S, Cacchiarelli D, Li VSW, Clevers H, Bonfanti P, Elvassore N, De Coppi P. Extracellular matrix hydrogel derived from decellularized tissues enables endodermal organoid culture. Nat Commun. 2019 Dec 11;10(1):5658. doi: 10.1038/s41467-019-13605-4. PMID: 31827102; PMCID: PMC6906306.

[24] Saldin LT, Cramer MC, Velankar SS, White LJ, Badylak SF. Extracellular matrix hydrogels from decellularized tissues: Structure and function. Acta Biomater. 2017 Feb;49:1-15. doi: 10.1016/j.actbio.2016.11.068. Epub 2016 Dec 1. PMID: 27915024; PMCID: PMC5253110.

[25] Dziki JL, Huleihel L, Scarritt ME, Badylak SF. Extracellular Matrix Bioscaffolds as Immunomodulatory Biomaterials. Tissue Eng Part A. 2017 Oct;23(19-20):1152-1159. doi: 10.1089/ten.TEA.2016.0538. Epub 2017 May 19. PMID: 28457179; PMCID: PMC6112165.

[26] Zhu Y, Hideyoshi S, Jiang H, Matsumura Y, Dziki JL, LoPresti ST, Huleihel L, Faria GNF, Fuhrman LC, Lodono R, Badylak SF, Wagner WR. Injectable, porous, biohybrid hydrogels incorporating decellularized tissue components for soft tissue applications. Acta Biomater. 2018 Jun;73:112-126. doi: 10.1016/j.actbio.2018.04.003. Epub 2018 Apr 10. PMID: 29649634; PMCID: PMC5985206.

[27] Tu Z, Han F, Zhu Z, Yu Q, Liu C, Bao Y, Li B, Zhou F. Sustained release of basic fibroblast growth factor in micro/nanofibrous scaffolds promotes annulus fibrosus regeneration. Acta Biomater. 2023 May 24:S1742-7061(23)00291-X. doi: 10.1016/j.actbio.2023.05.034. Epub ahead of print. PMID: 37230436.

[28] Koo YW, Lim CS, Darai A, Lee J, Kim W, Han I, Kim GH. Shape-memory collagen scaffold combined with hyaluronic acid for repairing intervertebral disc. Biomater Res. 2023 Mar 29;27(1):26. doi: 10.1186/s40824-023-00368-9. PMID: 36991502; PMCID: PMC10061910.

[29] Penolazzi L, Lambertini E, Bergamin LS, Roncada T, De Bonis P, Cavallo M, Piva R. MicroRNA-221 silencing attenuates the degenerated phenotype of intervertebral disc cells. Aging (Albany NY). 2018 Aug 20;10(8):2001-2015. doi: 10.18632/aging.101525. PMID: 30130742; PMCID: PMC6128426.

[30] Piccoli M., Urbani L., Alvarez-Fallas M. E., Franzin C., Dedja A., Bertin E., et al. (2016). Improvement of diaphragmatic performance through orthotopic application of decellularized extracellular matrix patch. Biomaterials 74 245–255. 10.1016/j.biomaterials.2015.10.005

[31] Jarrah RM, Potes MDA, Vitija X, Durrani S, Ghaith AK, Mualem W, Zamanian C, Bhandarkar AR, Bydon M. Alginate hydrogels: A potential tissue engineering intervention for intervertebral disc degeneration. J Clin Neurosci. 2023 Jul;113:32-37. doi: 10.1016/j.jocn.2023.05.001. Epub 2023 May 7. PMID: 37159956.

[32] Daly AC. Granular hydrogels in biofabrication - Recent advances and future perspectives. Adv Health Mater. 2023 Jun 14:e2301388. doi: 10.1002/adhm.202301388. Epub ahead of print. PMID: 37317658.

[33] Samantha L. Marshall, Timothy D. Jacobsen, Erik Emsbo, Archana Murali, Kevin Anton, Jessica Z. Liu, Helen H. Lu, and Nadeen O. Chahine Three-Dimensional-Printed Flexible Scaffolds Have Tunable Biomimetic Mechanical Properties for Intervertebral Disc Tissue Engineering ACS Biomaterials Science & Engineering 2021 7 (12), 5836-5849 DOI: 10.1021/acsbiomaterials.1c01326

[34] Angelozzi M, Penolazzi L, Mazzitelli S, Lambertini E, Lolli A, Piva R, Nastruzzi C. Dedifferentiated Chondrocytes in Composite Microfibers As Tool for Cartilage Repair. Front Bioeng Biotechnol. 2017 Jun 13;5:35. doi: 10.3389/fbioe.2017.00035. PMID: 28660185; PMCID: PMC5468460.

[35] Curley CJ, Dolan EB, Otten M, Hinderer S, Duffy GP, Murphy BP. An injectable alginate/extra cellular matrix (ECM) hydrogel towards acellular treatment of heart failure. Drug Deliv Transl Res. 2019 Feb;9(1):1-13. doi: 10.1007/s13346-018-00601-2. PMID: 30511249.

[36] Zheng K, Du D. Recent advances of hydrogel-based biomaterials for intervertebral disc tissue treatment: A literature review. J Tissue Eng Regen Med. 2021 Apr;15(4):299-321. doi: 10.1002/term.3172. Epub 2021 Mar 4. PMID: 33660950.

[37] Ju Y, Hu Y, Yang P, Xie X, Fang B. Extracellular vesicle-loaded hydrogels for tissue repair and regeneration. Mater Today Bio. 2022 Dec 21;18:100522. doi: 10.1016/j.mtbio.2022.100522. PMID: 36593913; PMCID: PMC9803958.

[38] Saravanou SF, Ioannidis K, Dimopoulos A, Paxinou A, Kounelaki F, Varsami SM, Tsitsilianis C, Papantoniou I, Pasparakis G. Dually crosslinked injectable alginate-based graft copolymer thermoresponsive hydrogels as 3D printing bioinks for cell spheroid growth and release. Carbohydr Polym. 2023 Jul 15;312:120790. doi: 10.1016/j.carbpol.2023.120790. Epub 2023 Mar 10. PMID: 37059530.

[39] de Vos, P., Hoogmoed, C.G. and Busscher, H.J. (2002), Chemistry and biocompatibility of alginate-PLL capsules for immunoprotection of mammalian cells. J. Biomed. Mater. Res., 60: 252-259. https://doi.org/10.1002/jbm.10060

[40] Ma K, Chen S, Li Z, Deng X, Huang D, Xiong L and Shao Z: Mechanisms of endogenous repair failure during intervertebral disc degeneration. Osteoarthritis Cartilage 27: 41-48, 2019

[41] Penolazzi L, Lambertini E, Scussel Bergamin L, Gandini C, Musio A, De Bonis P, Cavallo M, Piva R. Reciprocal Regulation of TRPS1 and miR-221 in Intervertebral Disc Cells. Cells. 2019 Sep 28;8(10):1170. doi: 10.3390/cells8101170. PMID: 31569377; PMCID: PMC6829335.

[42] Wangler S, Peroglio M, Menzel U, Benneker LM, Haglund L, Sakai D, Alini M, Grad S. Mesenchymal Stem Cell Homing Into Intervertebral Discs Enhances the Tie2-positive Progenitor Cell Population, Prevents Cell Death, and Induces a Proliferative Response. Spine (Phila Pa 1976). 2019 Dec 1;44(23):1613-1622. doi: 10.1097/BRS.0000000000003150. PMID: 31730570; PMCID: PMC6867676.

[43] Y. Song, S. Lu, W. Geng, et al., "Mitochondrial quality control in intervertebral disc degeneration," *Experimental Molecular Medicine*, vol. 53, n. 7, pp. 1124-1133, 2021.

[44] Shu-Hua Yang, Ming-Hsiao Hu, Chang-Chin Wu, Chih-Wei Chen, Yuan-Hui Sun & Kai-Chiang Yang (2019) CD24 expression indicates healthier phenotype and less tendency of cellular senescence in

human nucleus pulposus cells, Artificial Cells, Nanomedicine, and Biotechnology, 47:1, 3021-3028, DOI: 10.1080/21691401.2019.1642205

[45] Humphreys, MD, Ward, L, Richardson, SM, Hoyland, JA. An optimized culture system for notochordal cell expansion with retention of phenotype. JOR Spine. 2018; 1:e1028. https://doi.org/10.1002/jsp2.1028

[46] Richardson SM, Ludwinski FE, Gnanalingham KK, Atkinson RA, Freemont AJ, Hoyland JA. Notochordal and nucleus pulposus marker expression is maintained by sub-populations of adult human nucleus pulposus cells through aging and degeneration. Sci Rep. 2017 May 4;7(1):1501. doi: 10.1038/s41598-017-01567-w. PMID: 28473691; PMCID: PMC5431421.

[47] Wang D, Li Z, Huang W, Cao S, Xie L, Chen Y, Li H, Wang L, Chen X, Yang JR. Single-cell transcriptomics reveals heterogeneity and intercellular crosstalk in human intervertebral disc degeneration. iScience. 2023 Apr 19;26(5):106692. doi: 10.1016/j.isci.2023.106692. PMID: 37216089; PMCID: PMC10192848.

[48] Zhang S, Liu W, Chen S, Wang B, Wang P, Hu B, Lv X, Shao Z. Extracellular matrix in intervertebral disc: basic and translational implications. Cell Tissue Res. 2022 Oct;390(1):1-22. doi: 10.1007/s00441-022-03662-5. Epub 2022 Jul 6. PMID: 35792910.

Figure legends

Figure 1 Schematic overview of the experimental plan. De-differentiated human IVD cells, human macrophages (M1 polarized) and human IVD biopsies were respectively studied, by the specified techniques, in *in vitro* and *ex-vivo* experiments using Transwell™ culture system setup.

Figure 2 Photographs respectively showing: the PDMS negative molds used for the fabrication of the WJMs (A, B); the freshly prepared and ionically cross-linked millicylinders (i.e., before freeze drying) (C-E) and the freeze-dried samples. Photographs represent A075G3 (C and F), A075G15W15 (D and G) and A075W3 (E and H). For the specific composition of the imaged samples see Table 2.

Figure 3 Effect of the exposure to the indicated WJMs on the viability (upper photograph set), cytoskeletal arrangement (middle photograph set) and proliferation (lower graph) of IVD cells. Before the specific staining, cells were cultured in the presence of the indicated WJMs in a Transwell™ culture system setup for 72 h. Viability was determined by the live/dead cell test using merged images obtained by fluorescence microscopy; the green fluorescence indicates the presence of Calcein labelled live cells and the red fluorescence indicate the presence of dead cells stained with propidium iodide. The cytoskeletal organization was imaged by staining with Alexa Fluor 488 Phalloidin (resulting in a green fluorescence) and counterstaining with DAPI (resulting in a blue fluorescence). Scale bars correspond to 20 µm (upper photographs) and to 10 µm (lower photographs). Cell proliferation: IVD cells were cultured up to 15 days in the presence of WJMs, namely A075G3 (filled circles), A075G15W15 (filled squares) and A075W3 (filled diamond), for comparison, the cell proliferation of control cells is also reported (open circles). Data represent the average of three independent experiments (biological replicates) run in triplicate. (A075W3vs CTR, P=0.11, d2; 0.069, d5; 0.002, d10; 0.019, d15. A075W3vs A075G3, P=0.01, d2; 0.067, d5; 0.008, d10; 0.037, d15. A075W3vs A075G15W15, P=0.12, d2; 0.093, d5; 0.14, d10; 0.12, d15)

Figure 4 Effect of the exposure to the indicated WJMs on the migration ability of IVD cells measured by scratch assay. Optical photomicrographs represent a typical experimental result, showing the migration of the IVD cells after 72 h of cell culture. The bar corresponds to 50 µm. The histograms show the summary of experiments performed in triplicate and expressed as mean percentage of wound closure (±SD), the plotted values represent the difference between wound width at 0 and 72

h (*P=0.008, A075W3vs CTR; ° P = 0.0005, A075W3vs A075G3; ^ P =0.0009, A075W3vs A075G15W15; n = 3, biological replicates).

Figure 5 Effect of the exposure to the indicated WJMs on human macrophages (M1 polarized), after 48h of cell culture. The expression level of CD80 and CD86 pro-inflammatory surface markers were performed by flow cytometry. The plots report the percentage amount (with respect to the control cells) of CD80 and CD86. * P=0.002, A075W3 vs M1; ^ P=0.024, A075W3 vs A075G3). The contents of TNFα and IL12 of conditioned medium collected in the same experimental conditions were also evaluated. Data represent the mean ± SD (n=3, biological replicates).

Figure 6 Effect of the exposure to the indicated WJMs on IVD cells, as expression of pro-discogenic markers determined after 7 days of cell culture. The selected markers were collagen type II α1 chain (COL2a1), aggrecan (ACAN), (A); SRY-Box transcription factor 9 (SOX9), transcriptional repressor GATA binding 1 (TRPS1) and forkhead box O3 (FOXO3a), (B). The relative protein expression was evaluated by immunocytochemistry and representative optical photomicrographic fields after immunostaining are reported. Protein levels were quantified by densitometric analysis of immunostained cell pictures using ImageJ software; the plotted results are expressed as means of pixels per one hundred cells ± SD, analysed in triplicate (technical replicates) for each sample (* P=0.002, A075W3vsA075G3, A075G15W15vsA075G3; ^ P=0.001, A075W3vsCTR, A075G15W15vsCTR; n=4, biological replicates). Scale bars, 20 μm.

Figure 7 Effect of the exposure to the WJMs containing different amounts of DWJ on IVD cells, as expression of indicated markers determined after 7 days of cell culture. The selected markers were collagen type II α1 chain (COL2a1), aggrecan (ACAN), SRY-Box transcription factor 9 (SOX9), transcriptional repressor GATA binding 1 (TRPS1) and forkhead box O3 (FOXO3a). The relative protein expression was evaluated by immunocytochemistry and representative optical photomicrographic fields after immunostaining are reported. Protein levels were quantified by densitometric analysis of immunostained cell pictures using ImageJ software; the plotted results are expressed as fold change relative to control cells ± SD (COL2α1, P=0.001, A075W15, A075W3, A075W6v CTR; ACAN, P=0.048 A075W3vs A075W15; SOX9, P=0.001, A075W15, A075W3, A075W6vs CTR, P=0.0005, A075W15, A075W6vs A075w3, A075G15W15; TRPS1, P=0.012, A075W15 vsA075W3; FOXO3a,

P=0.01, A075W3, A075W6v CTR, P=0.005, A075W15, A075W6 vsA075W3; n=4, biological replicates). Scale bars, 10 µm.

Figure 8 Effect of A075W3 multifunctional millicylinder on organ IVD culture model. IVD tissue samples from 3 different donors (#14, #15 and #6) were incubated for 7 days in the presence of A075W3. The presence of CD24 positive cells was evaluated by flow cytometry; the expression of FOXO3a, SOD2 and TRPS1 was evaluated by immunohistochemistry. (A) Protein levels were quantified by densitometric analysis of immunostaining using ImageJ software and expressed as % of positive cells per area. The plotted results are expressed as means ± SD (n=5, technical replicates). All data points for replicates have been reported in the graphs. (B) Representative optical photomicrographic fields after immunostaining are reported (for each indicated marker, control on the left and A075W3, on the right). Scale bars, 20 µm.